

Fig. S1. (Related to figure 1) Characterization of *TFAP2AE1* expression, RNA-Seq quality control and enriched factor in-situ hybridization

(A) *Ex ovo* electroporation of *Tfap2aE1-GFP* shows enhancer activity in the dorsal neural folds (HH7), and in the early migrating (HH9-10) and late migrating (HH12) cranial neural crest. Scale bar 100 μm .

(B) Cross-section of a HH10 chicken embryo, showing that activity of the *Tfap2aE1-GFP* enhancer is specific to the neural crest. Scale bar 50 μm .

(C) Principal component analysis of both neural crest (GFP+) and whole embryo (GFP-) RNA-Seq samples. Principal component 1 (33% of variance) separates both conditions by developmental time, while principal component 2 (25% of variance) separates neural crest and whole embryo samples.

(D) Whole mount *in situ* hybridizations for significantly enriched factors expressed in the neural crest lineage. Scale bar 100 μm .

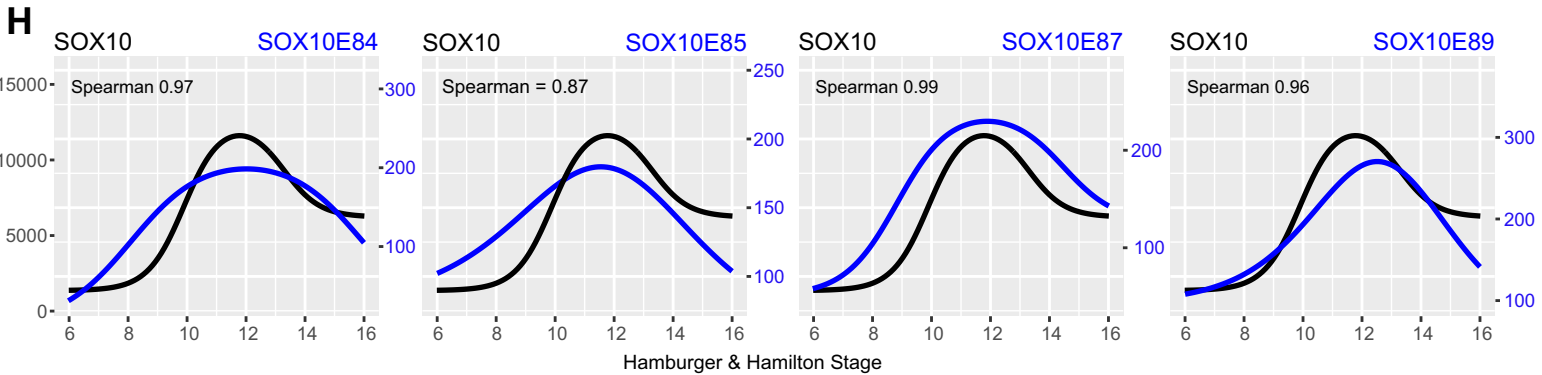
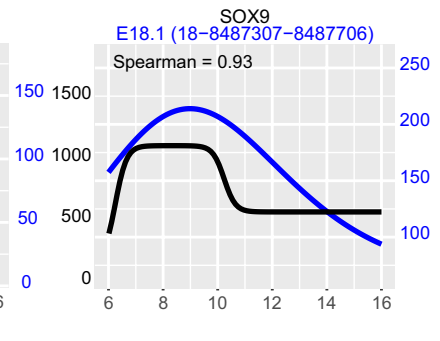
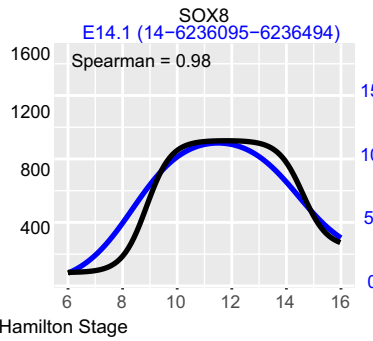
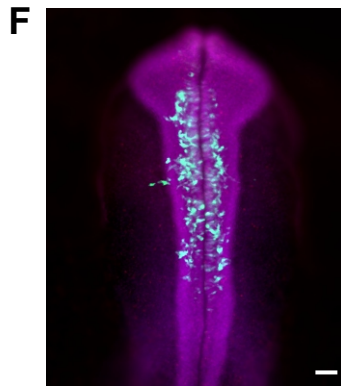
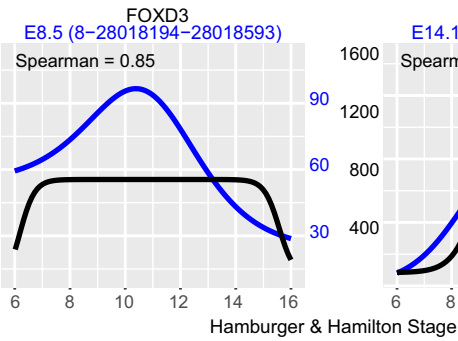
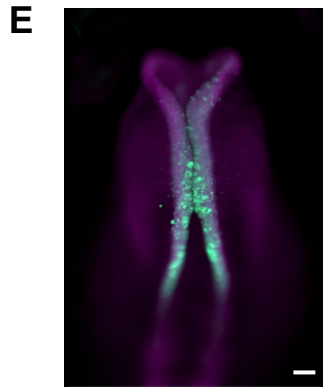
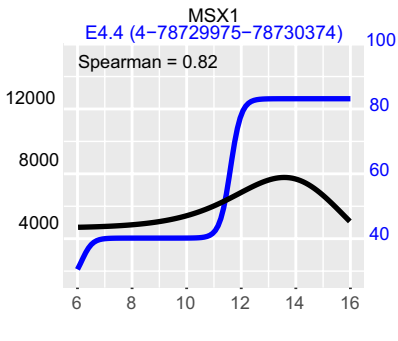
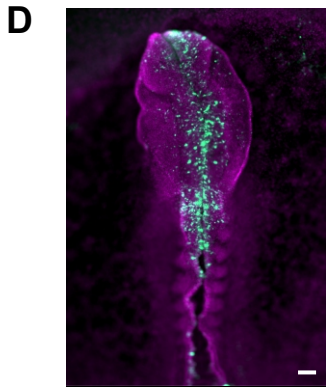
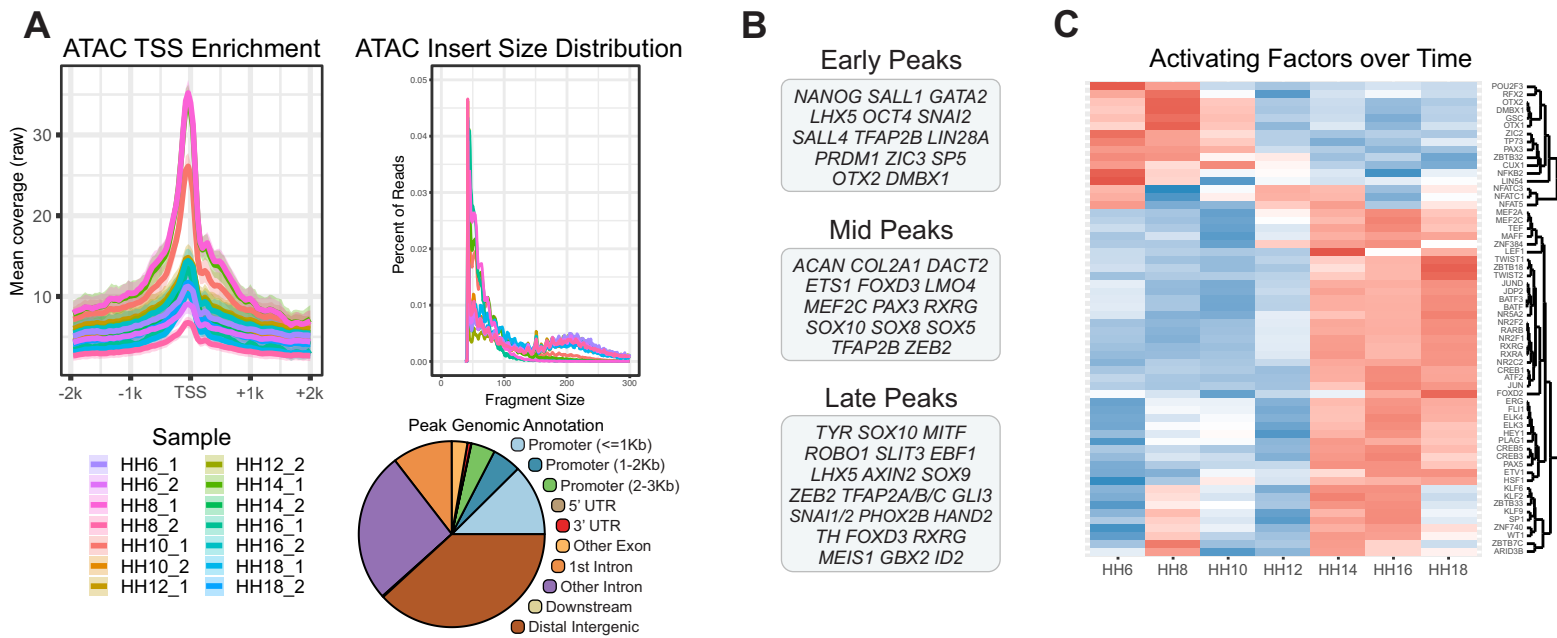


Fig. S2 (Related to figure 2) ATAC-Seq quality control, DiffTF and chromVAR integration, and in-vivo verification of peak to gene correlation analysis.

(A) Quality control plots for chicken ATAC-Seq samples. Left, an ATAC-Seq TSS enrichment plot with mean coverage around the transcription start site and +/- 2 kilobases of all genes. Right top, the insert size distribution plot. Fragments < 120bp indicate nucleosome free binding. Right bottom, a genomic annotation plot of all ATAC-Seq peaks, demonstrating promoter, intronic, and distal intergenic enrichment.

(B) Genes identified from peak to gene correlation analysis in the early, mid, and late peak groups.

(C) A heatmap of DiffTF classified activating transcription factors variability over time. Transcription factors are clustered hierarchically, resulting in two large clusters.

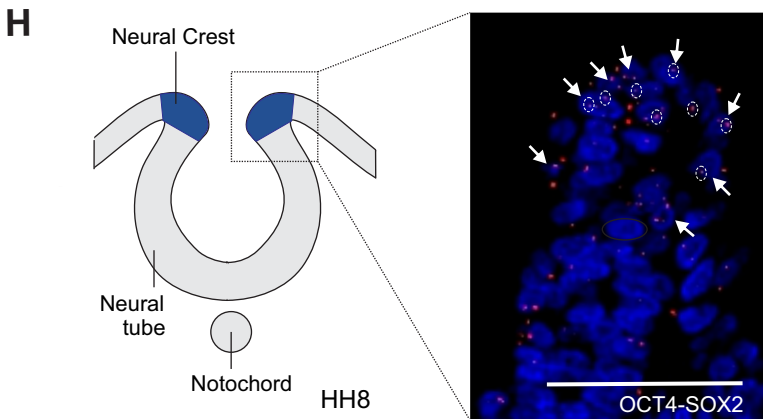
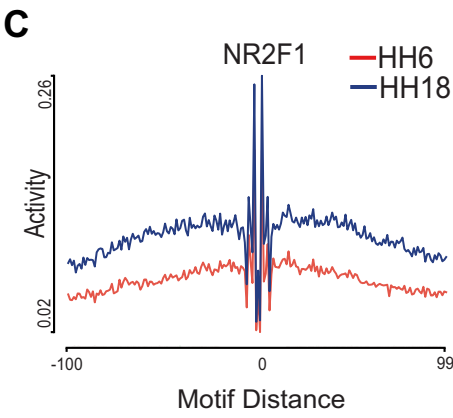
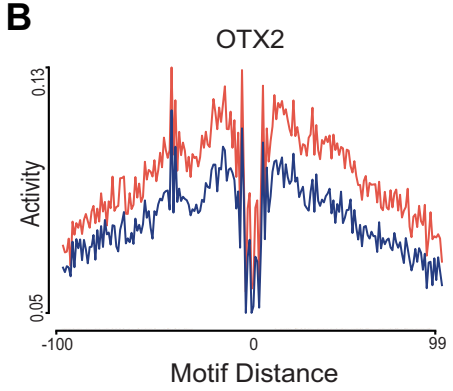
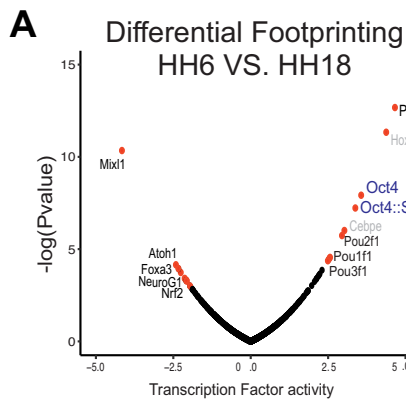
(D) *Ex ovo* electroporation of the *MSX1 E4.4* enhancer and the correlation plot between the gene (black) and the enhancer (blue). Scale bar 100 μm .

(E) *Ex ovo* electroporation of the *FOXD3 E8.5* enhancer and the correlation plot between the gene (black) and the enhancer (blue). Scale bar 100 μm .

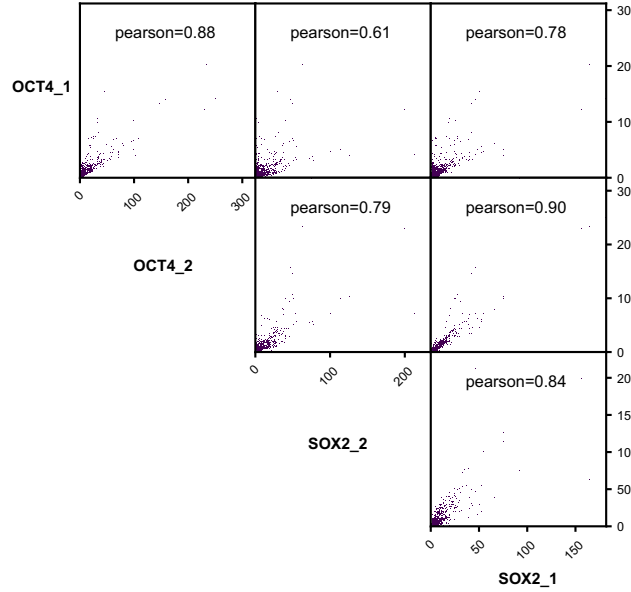
(F) *Ex ovo* electroporation of the *SOX8 E14.1* enhancer and the correlation plot between the gene (black) and the enhancer (blue). Scale bar 100 μm .

(G) *Ex ovo* electroporation of the *SOX9 E18.1* enhancer and the correlation plot between the gene (black) and the enhancer (blue). Scale bar 100 μm .

(H) Correlation plots for *SOX10* and four associated enhancer regions, demonstrating that this method can robustly capture known enhancers.



D CUT&RUN Correlation



E Motif Enrichment & Fragment Size

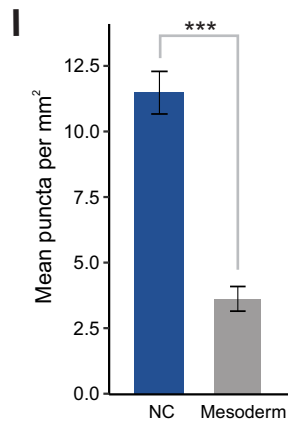
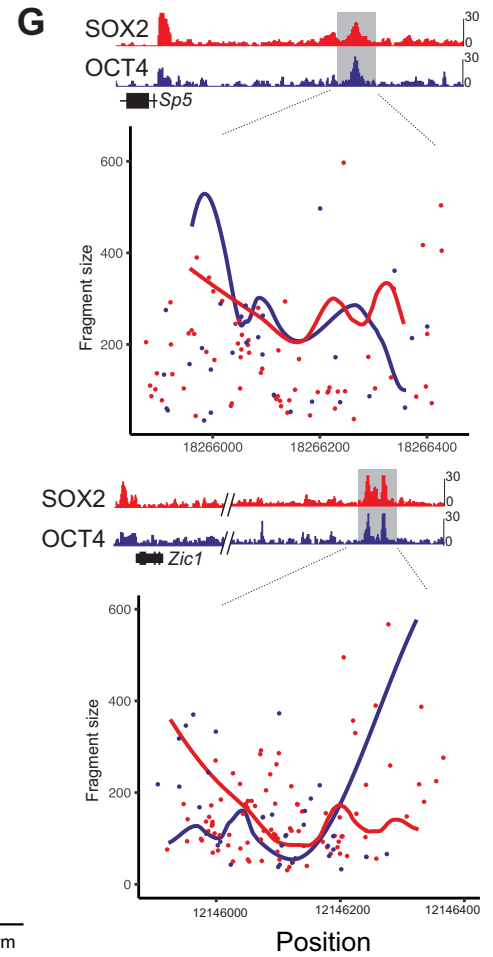
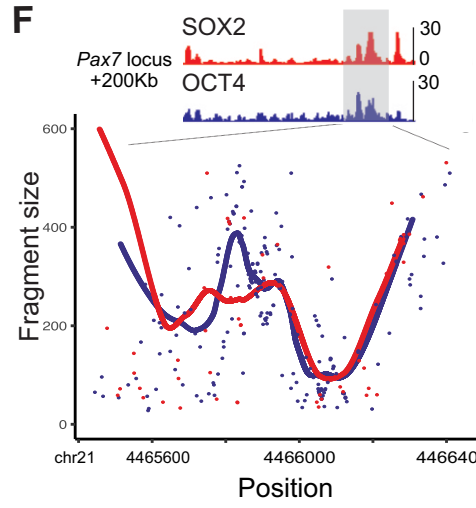
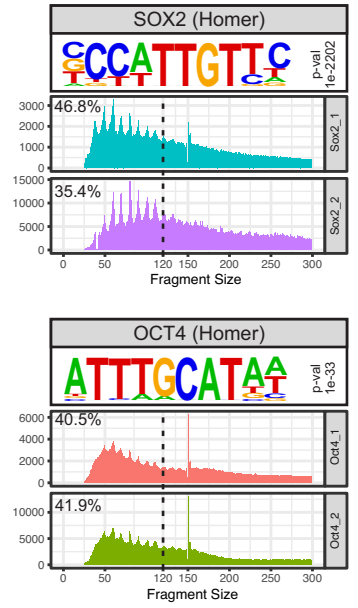


Fig. S3 (Related to figure 3) CUT&RUN quality control, transcription factor footprinting and EChO analysis.

(A) Differential footprinting analysis between HH6 and HH18 ATAC-Seq samples shows OCT4 and OCT4-SOX2 are two of the top motifs whose footprint are enriched in HH6.

(B) A motif footprinting plot for OTX2, showing enrichment in HH6 ATAC-Seq samples.

(C) A motif footprinting plot for NR2F1, showing enrichment in HH18 ATAC-Seq samples.

(D) Bin-wise correlation quality control plots for the OCT4 and SOX2 CUT&RUN libraries.

(E) Motif enrichment (from Homer) and fragment size distribution quality control plots for the SOX2 and OCT4 CUT&RUN libraries.

(F) A genome browser plot of a putative regulatory region for *SP5*. EChO analysis of OCT4 and SOX2 CUT&RUN data shows co-binding events (local minima).

(G) A genome browser plot of a putative regulatory region for *ZIC1*. EChO analysis of OCT4 and SOX2 CUT&RUN data shows co-binding of the two factors in the *ZIC1* locus.

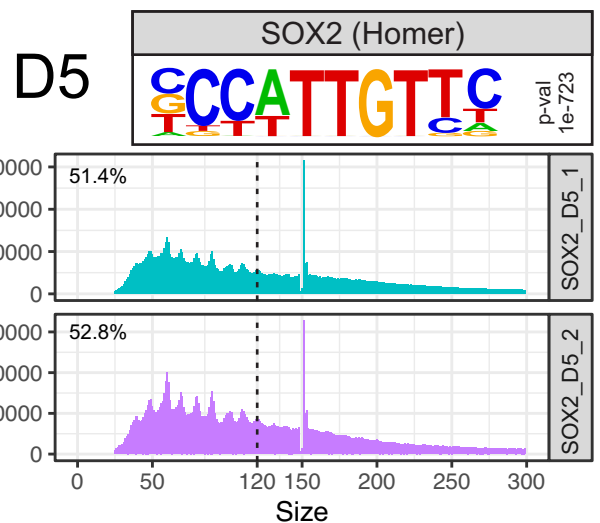
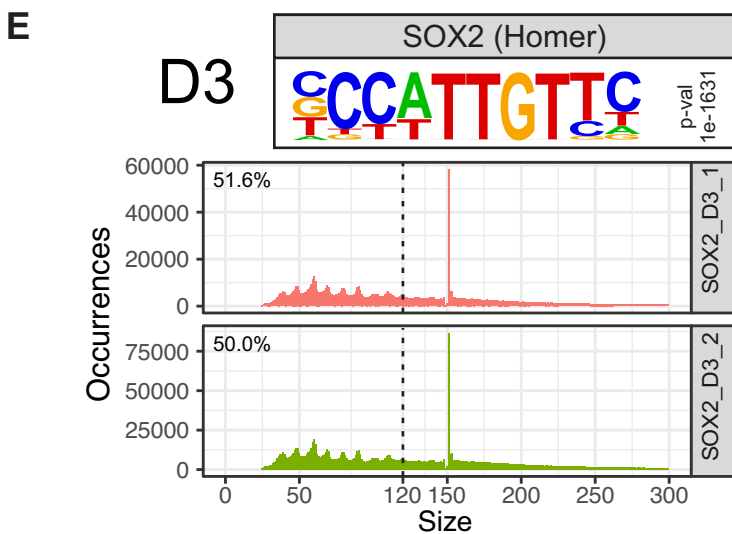
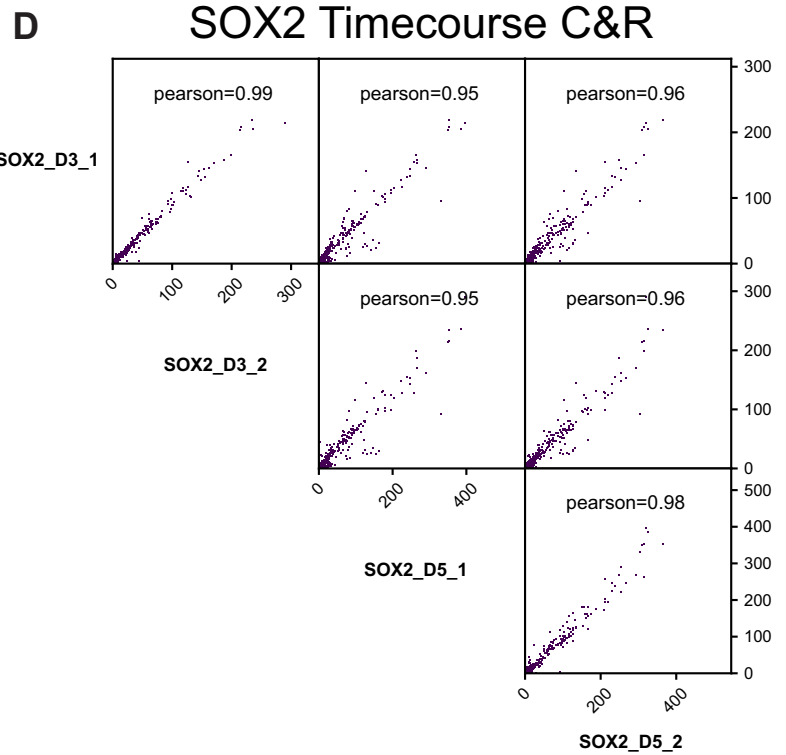
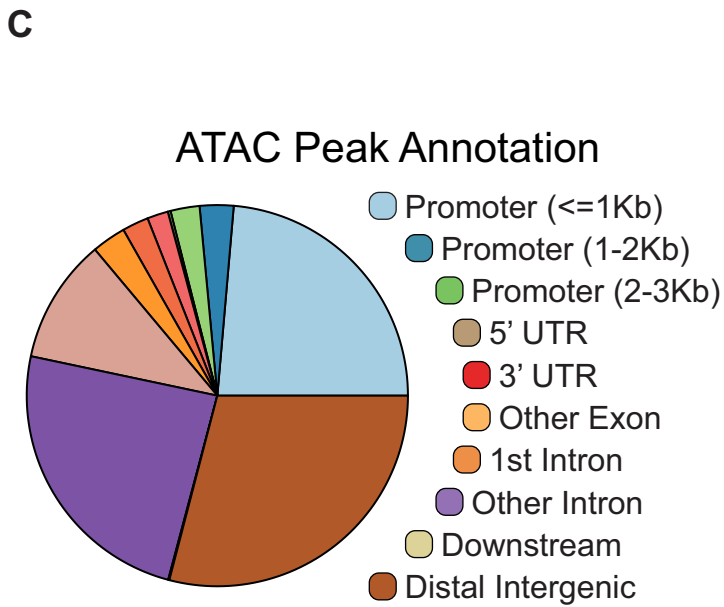
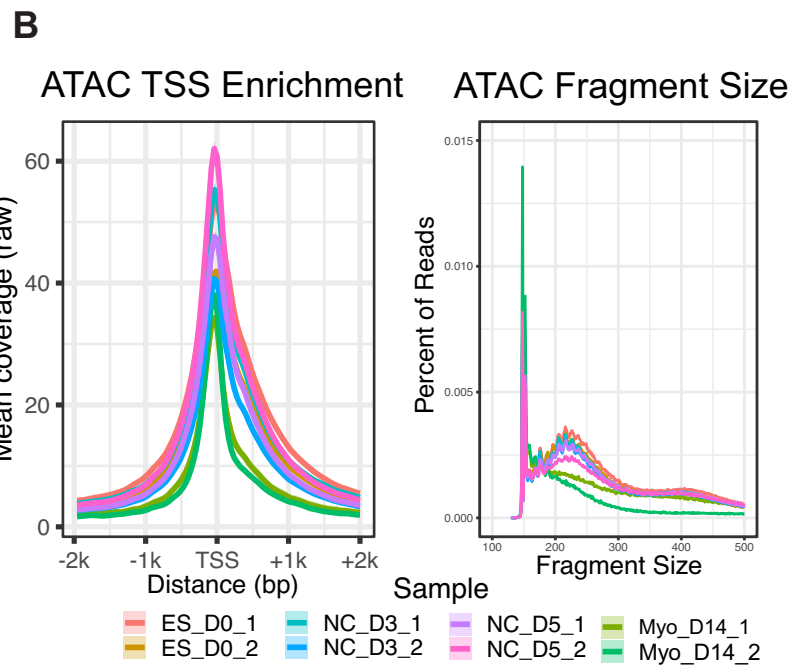
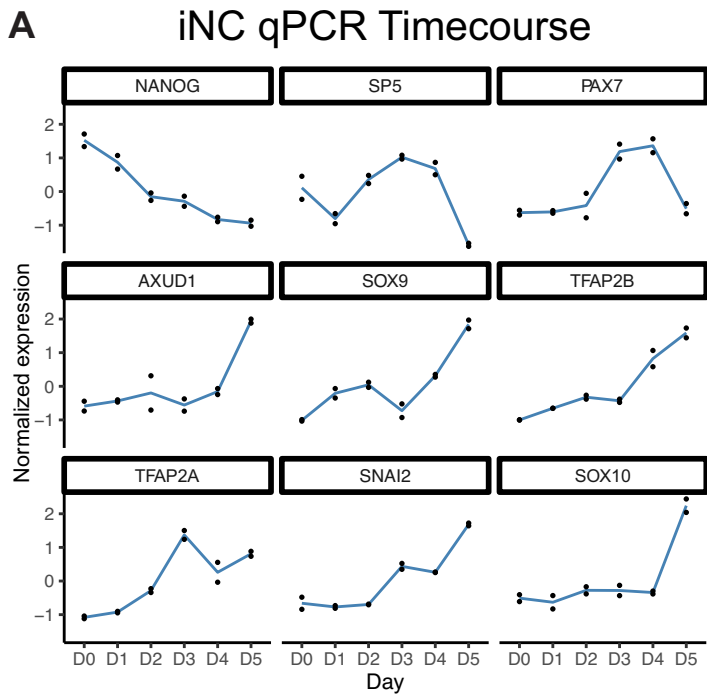


Fig. S4. (Related to figure 4) hiNCC expression characterization and genomic library quality control.

(A) qPCR expression plots for various genes during the human embryonic stem cell (D0) to induced neural crest cell (D5) differentiation process.

(B) Quality control plots for ATAC-Seq performed across the iNC time course. Left, an ATAC-Seq TSS enrichment plot with mean coverage around the transcription start site and +/- 2 kilobases of all genes. Right, the insert size distribution plot. Fragments < 120bp indicate nucleosome free binding.

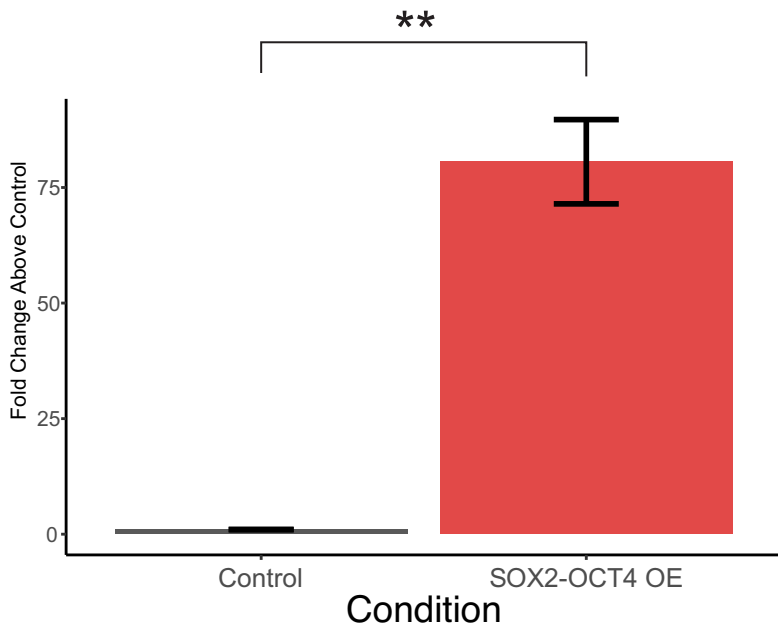
(C) Genomic annotation of all ATAC-Seq peaks, demonstrating enrichment at promoters, introns, and distal intergenic regions.

(D) Bin-wise correlation quality control plot for SOX2 CUT&RUN for D3 and D5 iNC CUT&RUN libraries.

(E) Motif enrichment for SOX2 (from Homer) and fragment size distribution for the D3 and D5 iNC CUT&RUN libraries.

A

SOX2 Expression in SOX2-OCT4 OE



B

Cell Death and Proliferation in SOX2-OCT4 OE

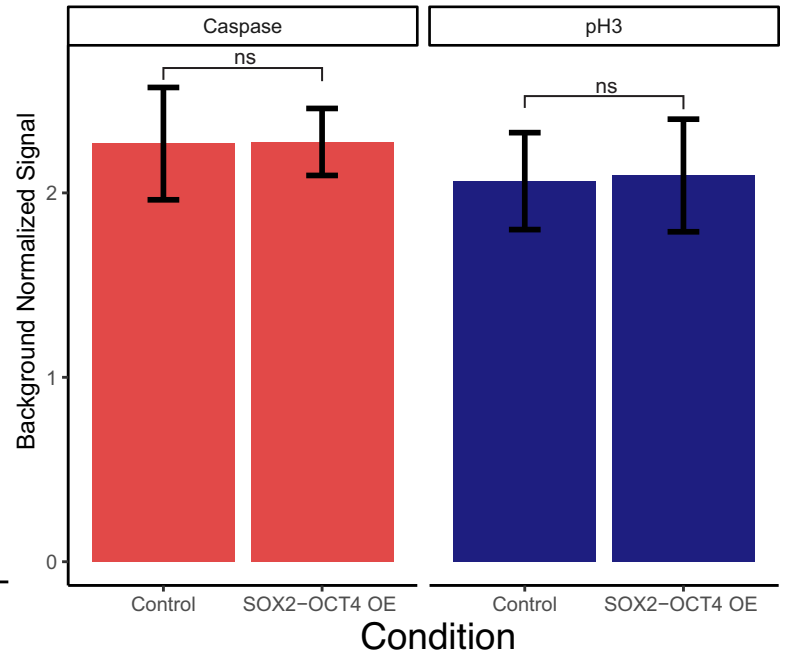


Fig. S5. (Related to figure 5) Quality control of SOX2/OCT4 in-vivo overexpression.

(A) Verification of SOX2 overexpression via qPCR for the SOX2-OCT4 overexpression experiment. qPCR was performed with five independent biological replicates with three technical replicates. SOX2-OCT4 OE condition had significantly higher (**, p-val 0.018) from a student's two-sided t-test.

(B) Quantification of immunohistochemistry for cell death (Caspase) and proliferation (pH3) in control versus SOX2-OCT4 overexpression conditions (ns, p-val > 0.05).

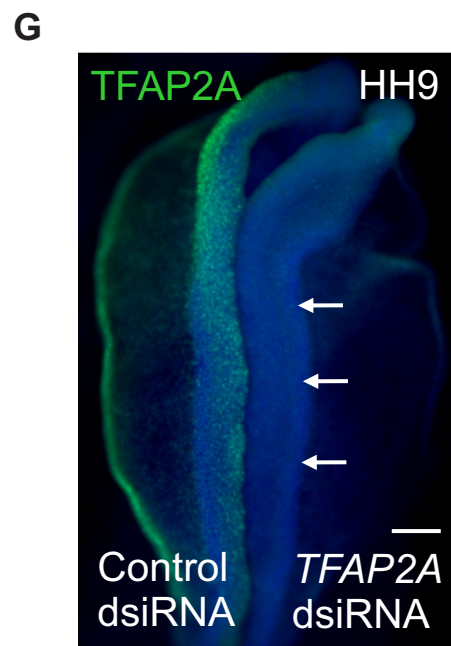
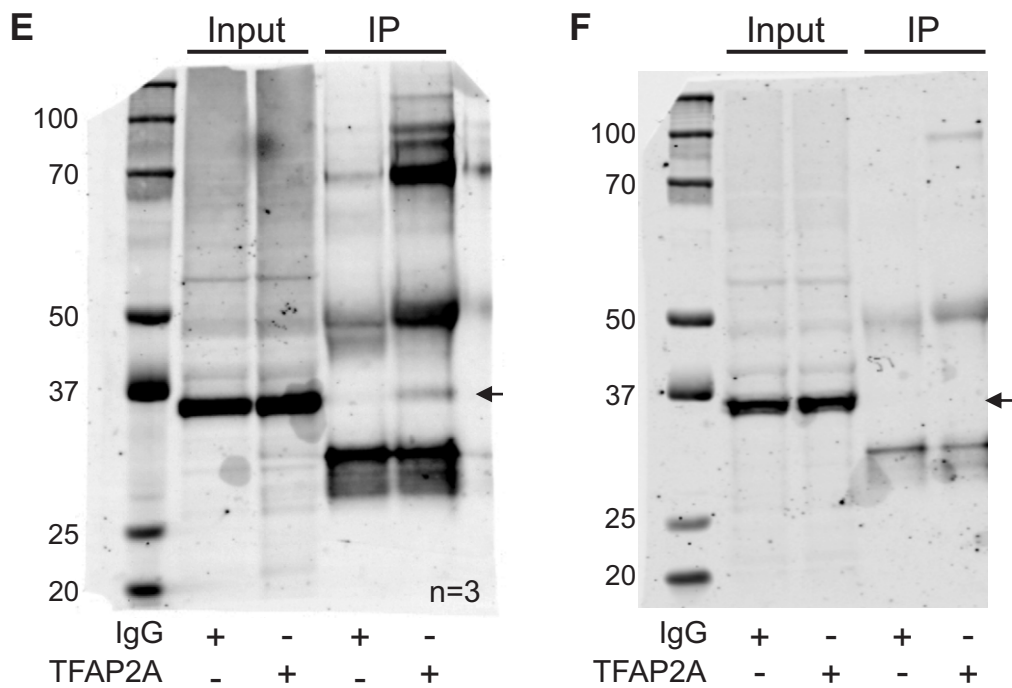
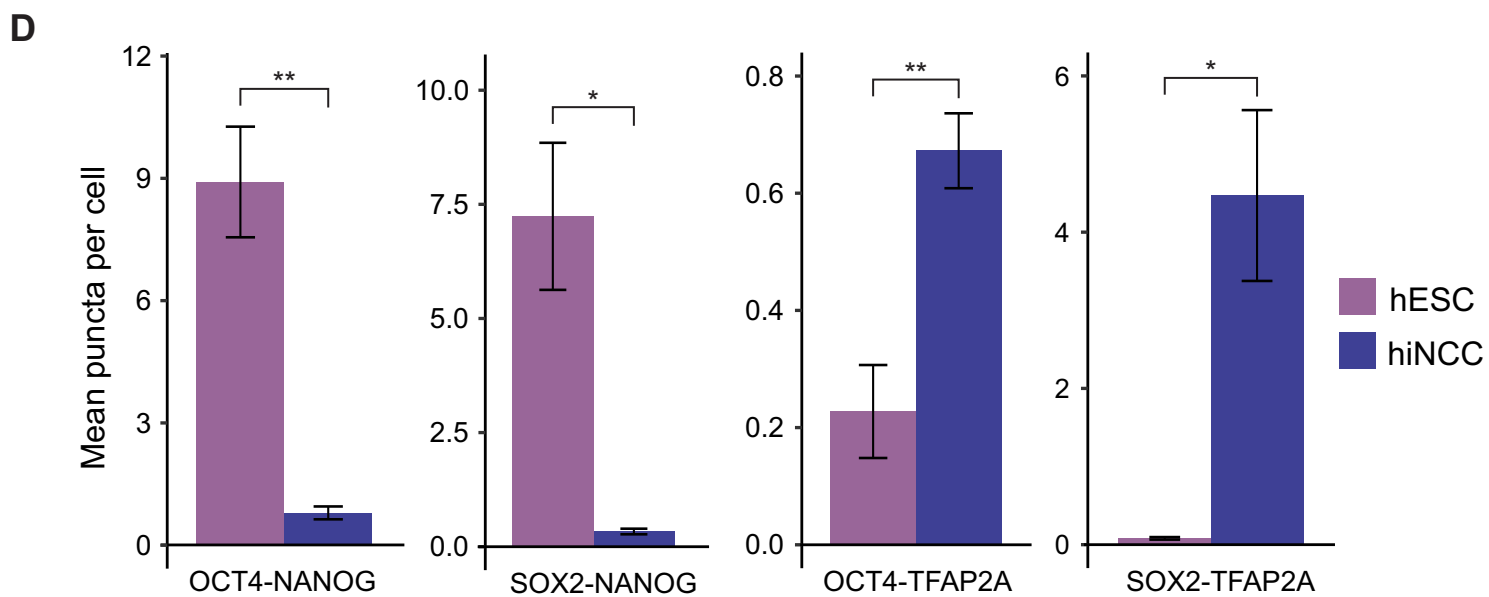
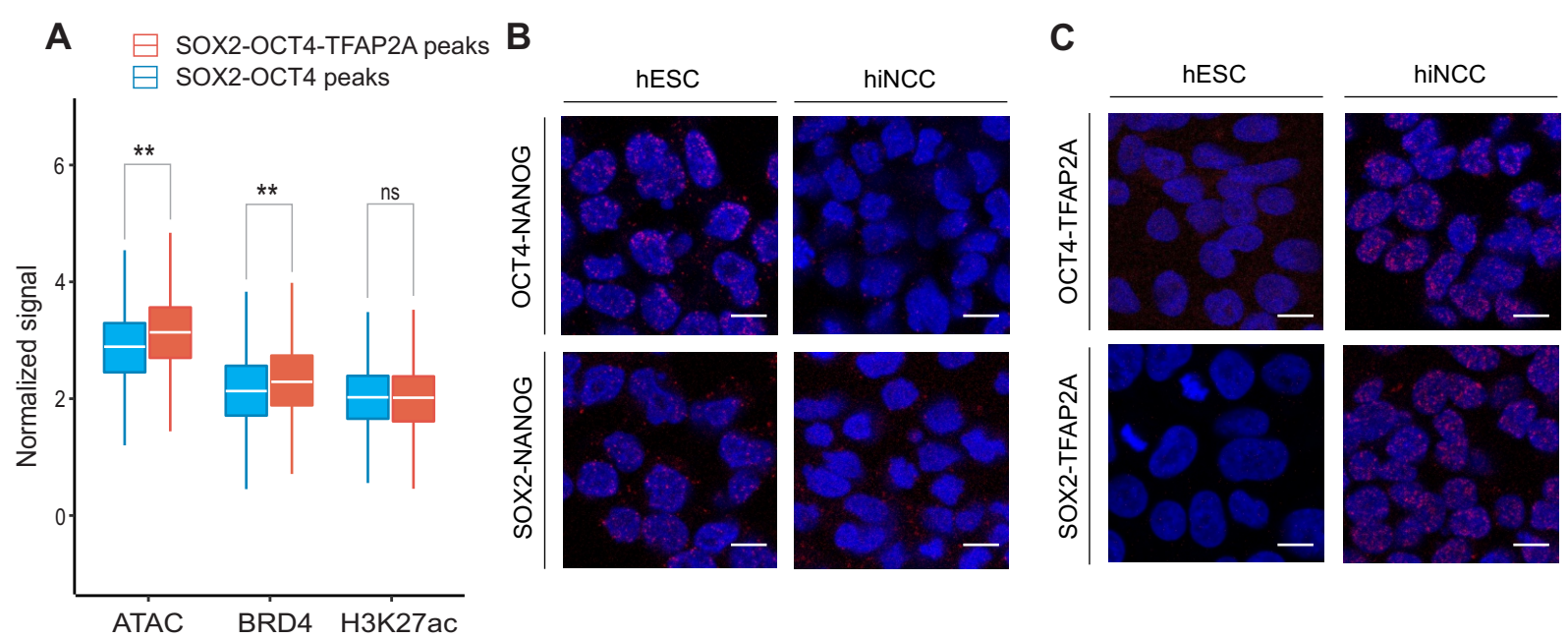


Fig. S6. (Related to figure 6) Endogenous Co-IP, TFAP2A dsiRNA validation, and proximity ligation assays.

(A) Boxplot showing that ATAC signal and BRD4 binding is higher in peaks bound by all 3 factors than those only bound by SOX2 and OCT4. H3K27ac signal at these regions was not significantly different.

(B) Proximity Ligation Assays (PLAs) for SOX2/OCT4-NANOG interactions. Positive interactions appear as nuclear, red puncta. Scale bar 10 μm .

(C) Proximity Ligation Assays (PLAs) for SOX2/OCT4-TFAP2A interactions. Positive interactions appear as nuclear, red puncta.

(D) Quantification of parts D&E. Samples were compared using a single tailed Student's t-test (* p-val < 0.05; ** p-val < 0.01)

(E) A western blot for SOX2 in an endogenous (chicken) co-immunoprecipitation assay. Under IP conditions, pulling down with TFAP2A results in detection of SOX2.

(F) A western blot for SOX2 in an endogenous (human embryonic stem cell) co-immunoprecipitation assay. Pulldown of TFAP2A is unable to recover SOX2 in D0 human ESCs.

(G) A HH9 embryo that has been bilaterally transfected with the *TFAP2A* dsiRNA on the right side of the embryo and immunostained for the TFAP2A protein. Scale bar 100 μm .

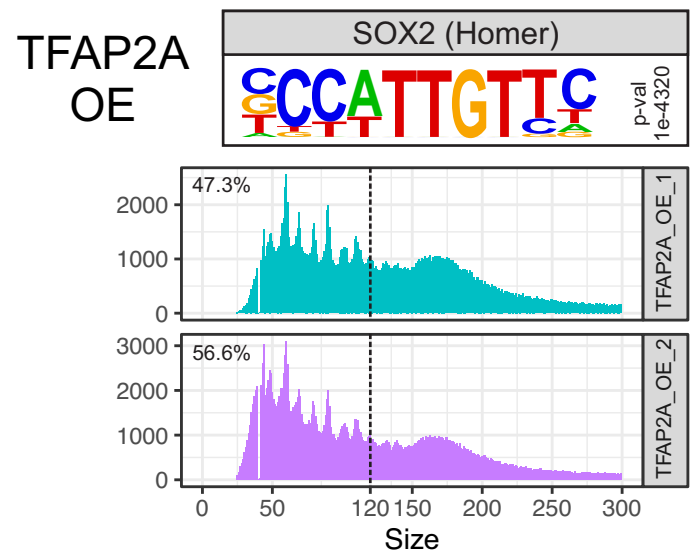
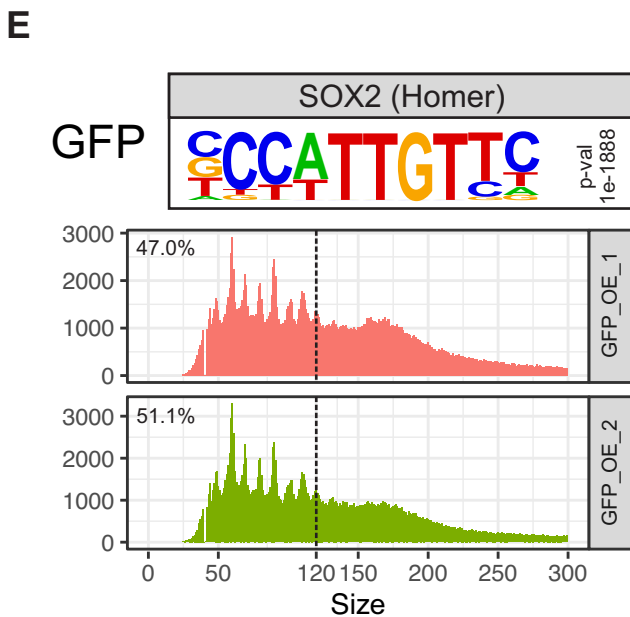
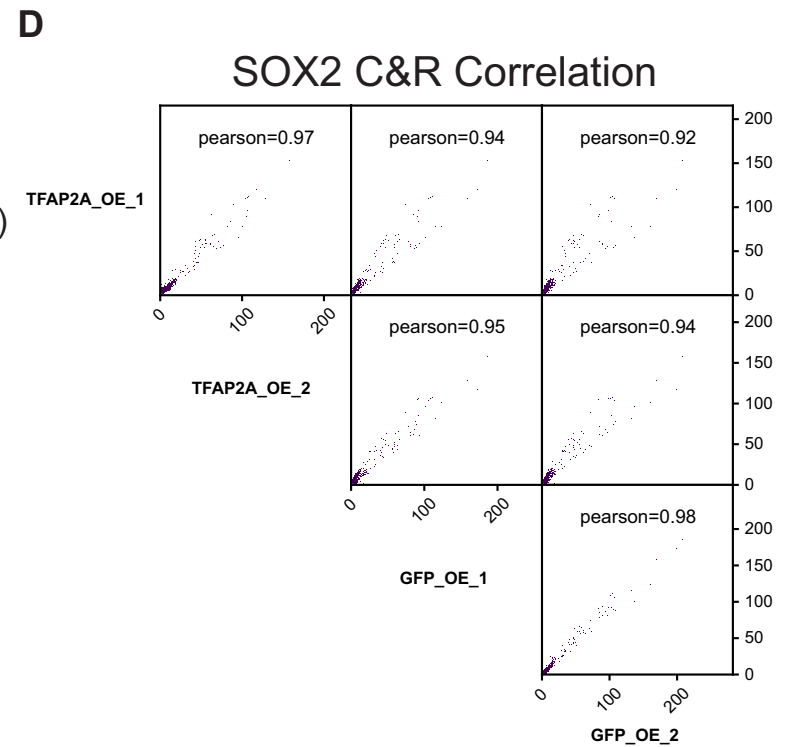
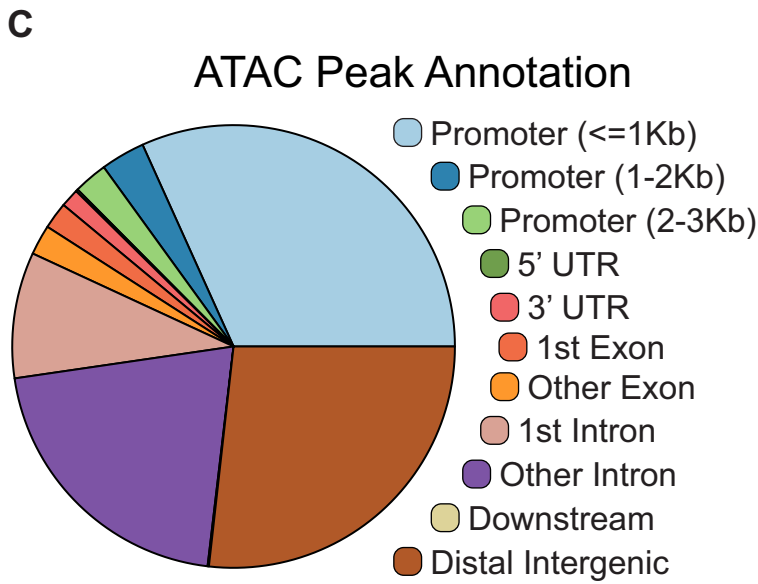
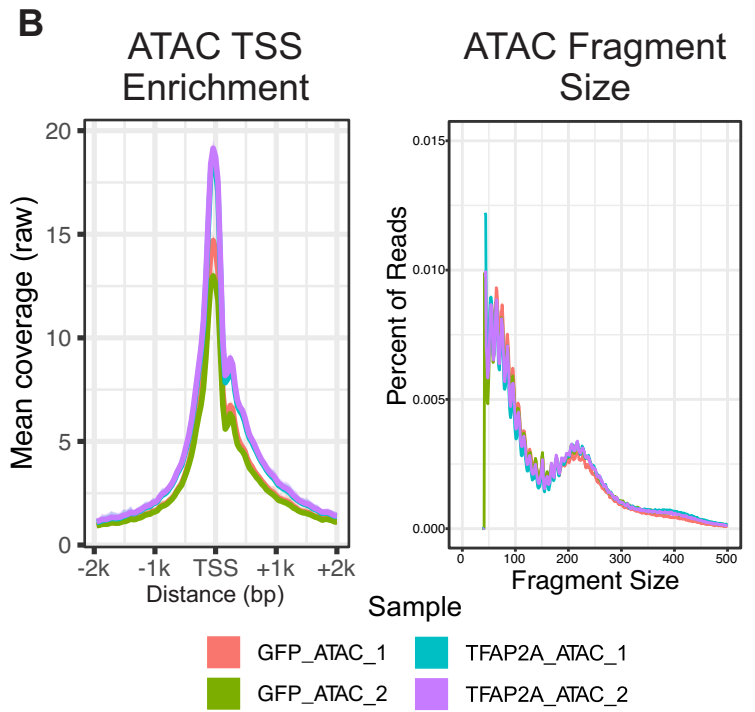
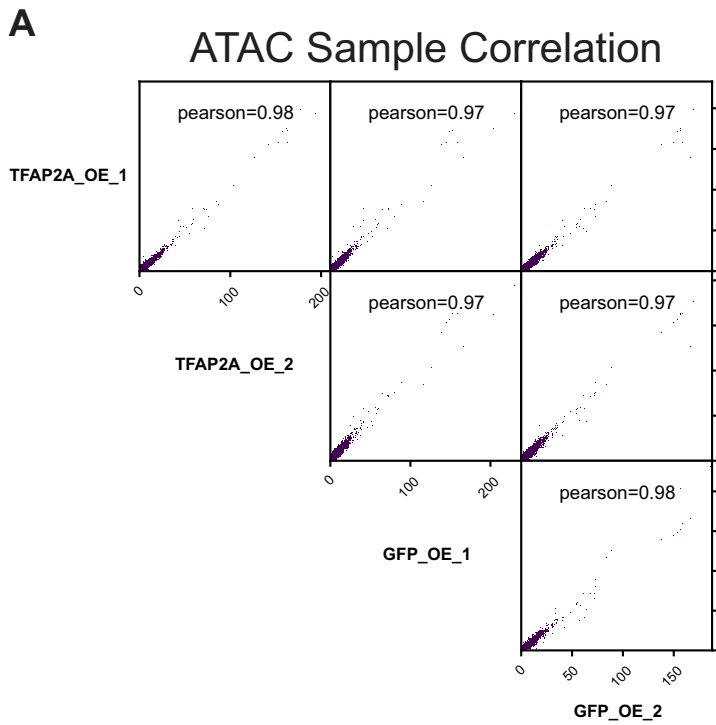


Fig. S7. (Related to figure 7) Quality control of genomic datasets in hESCs with TFAP2A and GFP overexpression.

(A) Bin-wise correlation quality control plots for TFAP2A and GFP overexpression ATAC libraries.

(B) Quality control plots for TFAP2A and GFP overexpression ATAC-Seq libraries. Left, an ATAC-Seq TSS enrichment plot with mean coverage around the transcription start site and +/- 2 kilobases of all genes. Right, an insert size distribution plot demonstrating nucleosome patterning.

(C) A genomic annotation plot for ATAC-Seq peaks, with strong enrichment in promoters, introns, and distal intergenic regions.

(D) A bin-wise correlation quality control plot for the TFAP2A and GFP overexpression SOX2 CUT&RUN libraries.

(E) SOX2 motif enrichment (from Homer) and fragment size distribution for TFAP2A and GFP overexpression CUT&RUN libraries.